Regenerative 40 Gbit/s wavelength converter based on similariton generation

Christophe Finot, Stéphane Pitois, Guy Millot

Regenerative 40-Gb/s wavelength converter based on similariton generation

C. Finot, S. Pitois and G. Millot

Laboratoire de Physique de l'Université de Bourgogne, Unité Mixte de Recherche CNRS 5027, 9 avenue A. Savary, B.P. 47 870, 21078 Dijon, France

Abstract

In this paper, we present an all-optical regeneration technique based on spectral filtering of self-similar parabolic pulses (similaritons). In particular, we demonstrate numerically and experimentally that ghost-pulses, which occur in the zero bit slots of telecommunication pulse trains, can be effectively suppressed. These results are obtained with a 40-Gb/s pulse train.

OCIS codes: 060.4510, 060.4370, 190.5530.

In strongly pulse-overlapped return-to-zero fiber transmission systems, a major limitation is introduced by intra-channel four-wave mixing which manifests itself by the generation of ghost-pulses in zero bit slots[1] and results in a significant increase of the bit-error rate. Several methods have been proposed to regenerate high bit rate pulse trains and to reduce noise and ghost-pulse energy at the end of transmission lines. These methods include wavelength converters based on cross-phase modulation,[2] spectral slicing of self-phase modulation (SPM) broadened spectrum,[3-5] four-wave mixing[6] and nonlinear optical loop mirror.[7]

In this Letter we propose an alternative method based on similariton generation in optical fiber amplifiers. Similaritons, or self-similar parabolic pulses, have been observed experimentally in rare-earth-doped fiber[8,9] and Raman[10] amplifiers. Similaritons represent particularly interesting solutions of the nonlinear Schrödinger equation (NLSE) with gain and normal dispersion. The similariton temporal and spectral intensities are both characterized by smooth linearly-chirped parabolic shapes, towards which, any arbitrary input pulse of given energy will converge, irrespective of its specific pulse profile or duration. Furthermore, the similariton chirp is independent of the input pulse energy and depends only on the gain and dispersion of the amplifier. These remarkable properties have been successfully exploited for different applications such as pulse compression,[8,9] pulse synthesis,[11] or high-power ultrashort fiber laser.[12] Here, we take advantage of the similariton properties to regenerate a 40-Gb/s pulse train at the end of a transmission line. The basic idea is to transform the initial signal pulses into similaritons and to subsequently slice and dechirp the broad spectrum of the similaritons by means of a frequency-shifted filter and a dispersion compensating fiber.

Let us first consider the evolution of a pulse train in the normal-dispersion regime of a fiber with distributed gain, provided either by Raman or Erbium pumping. Evolution of the slowly varying envelope $E(z,t)$ of the electric field in such an amplifier can be described by the standard NLSE with distributed gain $g(z)$. For an amplification with a constant longitudinal gain g, it has been demonstrated that the NLSE admits an asymptotic solution which can be written as:[13]

$$E(z,t) = A_o \exp(gz/3)\sqrt{1 - \left(\frac{t}{T(z)}\right)^2} \exp\left[i\left(\varphi(z) - \frac{C}{2}t^2\right)\right],\ |t| \leq T(z) \quad (1)$$

with $E(z,t) = 0$ for $|t| > T(z)$. Here, $\varphi(z)$ is a phase term, $C = g/3\beta_2$, A_o is a constant amplitude term $A_o = 1/2\left(gU_{in}\big/\sqrt{\gamma\beta_2/2}\right)^{1/3}$ where U_{in} is the initial pulse energy, β_2 and γ are the group-velocity dispersion and nonlinear coefficients, respectively, and T(z) is the temporal width given by $T(z) = (6A_o/g)\sqrt{\gamma\beta_2/2}\exp(gz/3)$. This solution describes a self-similar pulse with a parabolic shape and a linear chirp. Such similariton pulses are generated asymptotically, independently of the input specific pulse shape and the output pulse parameters are only determined by the input energy.[14] The most important feature here is that, during the amplification process, the spectrum of the amplified pulse broadens and tends to have a parabolic shape with a strictly linear chirp:

$$\tilde{E}(z,\omega) = \mathrm{A_o}/\sqrt{\mathrm{C}}\ \exp(gz/3)\sqrt{1 - \left(\frac{\omega}{\Omega(z)}\right)^2} \exp\left[i\left(\psi(z) - \frac{\omega^2}{2\mathrm{C}}\right)\right],\ |\omega| \leq \Omega(z) \quad (2)$$

with $\tilde{E}(z,\omega) = 0$ for $|\omega| > \Omega(z)$, and $\psi(z)$ is a phase term. The pulse spectral width increases exponentially with the propagation distance and only depends on the initial pulse energy and fiber parameters: $\Omega(z) = \mathrm{A_o}\sqrt{2\gamma/\beta_2}\ \exp(gz/3)$. The regeneration mechanism presented in this paper is essentially based on these remarkable properties.

We consider first the self-similar parabolic amplification of a 40-GHz pulse train containing only "ones". The NLSE with distributed gain $g(z)$ has been solved numerically using the standard split-step Fourier propagation method. Without any loss of generality, in the following we will focus our attention on the backward Raman amplification configuration with a pump power of 1.8 W. The Raman amplifier consists of a standard non-zero dispersion shifted fiber (NZ-DSF) with the following parameters: fiber length L = 1800 m, dispersion D = -1.8 ps/nm/km, slope S = 0.07 ps/nm^2/km and linear losses α = 0.3 dB/km. For convenience, these parameters correspond to those used in the experiment discussed below. Figure 1(a1) shows the spectrum of the pulse train at the amplifier input. Self-similar amplification in the NZ-DSF leads to spectral broadening, while keeping a smooth spectral shape, as illustrated in Figs. 1(b1) and (c1) for an average input power P_{av} of 40 mW and 230 mW, respectively. We verify that the initial Gaussian pulse train [Fig. 1(a2)] transforms itself into a parabolic pulse train as the input average power increases [Figs. 1(b2) and (c2)]. Basically, our regenerative method is based on this energy-dependent spectral broadening to discriminate high-energy pulses ("ones") from low-energy pulses ("ghost-pulses") using a bandpass filter whose center frequency is shifted with respect to the original signal carrier frequency. Indeed, high-energy input pulses transform themselves into similaritons with a broad and smooth spectrum and are thus partially passed by the filter, whereas low-energy input pulses, which have not yet reached the self-similar asymptotic regime, remain spectrally narrow and are thus rejected by the filter. The filter transmission profile is represented in Fig. 1 as dashed line.

We emphasize that the similariton-based regenerator presents several remarkable properties which differentiate it from the SPM-based regenerator.[3] Indeed, similariton-broadened spectrum has a smooth profile, whereas SPM-broadened spectrum is generally accompanied by oscillatory structures covering the entire frequency range, and fiber parameters should be carefully optimized to minimize these spectral ripples.[5] Moreover, the spectrum and chirp obtained by SPM both depend on the details of the initial pulse (shape, chirp and energy), leading to amplitude and time fluctuations of the regenerated pulses.[4] In particular, pulses with different initial intensities acquire different amounts of SPM-induced chirp at the fiber output, resulting in timing jitter.[4] In contrast, the similariton-based spectral broadening only depends on the input pulse energy, and the similariton-induced chirp only depends on the amplifier parameters, so that amplitude and timing jitters are strongly reduced. On the other hand, chirp compensation at the similariton regenerator output can be simply performed since all filtered pulses have identical chirp profiles.

To study in more details the properties of the similariton-based regenerator, we consider now a pseudo-random bit sequence (PRBS) which has propagated in an usual practical transmission line. Figures 2(a) and (b) represent the eye diagram of this pulse train at the input and output of the transmission line, respectively. Due to nonlinear pulse to pulse interactions, ghost-pulses have been generated during propagation through the transmission line. Figure 2(c) illustrates the pulse train generated at the similariton generator output. The eye diagram after filtering is shown in Fig. 2(d). The average power at the regenerator input was 100 mW and the filter offset was 100 GHz. Ghost pulses and noise are now reduced by more than 25 dB, compared to the "ones" level. On the other hand, a 12 % reduction of the timing jitter was calculated between the PRBS train before regeneration [Fig. 2(b)] and the corresponding PRBS train obtained at the output of the similariton-based regenerator [Fig. 2(d)].

The experimental set-up is shown in Fig. 3. The 40-Gb/s pulse train was obtained by temporally multiplexing two 20-GHz pulse trains emitted near 1550 nm from a home-built laser source. One of the two 20-GHz pulse trains corresponds to the "ones" whereas the other represents artificial ghost pulses. The 20-GHz source generates transform-limited pedestal-free pulses with 9-ps duration by means of the technique of multiwave mixing temporal compression of an initial dual-frequency beat signal[15] in a standard single mode fiber (SMF-28). A variable attenuator was used to control the peak power ratio between the "ones" and the ghost pulses. The 40-Gb/s signal pulses were subsequently amplified to the desired average power level by an erbium-doped fiber amplifier (EDFA) and sent into the 1800-m NZ-DSF with normal dispersion. A 1.8-W cw beam delivered by a 1450-nm Raman laser was injected into the NZ-DSF in a backward configuration. A Gaussian filter with a center wavelength at 1548.6 nm and a 3-dB bandwidth of 60 GHz was used at the similariton generator output to select only a part of the similariton spectrum. Chirp compensation of the regenerated signal pulses was achieved by means of a short piece of standard single mode fiber. The regenerated and dechirped signal pulse train was characterized by means of a second-harmonic optical autocorrelator.

Figure 4(a) shows the autocorrelation traces of the 40-Gb/s pulse train obtained at the similariton generator input (circles) and output for different values of the filter offset Δf (dashed, dotted and solid lines). For Δf = 200 GHz (solid line), we clearly observe that the ghost-pulses have been successfully suppressed whereas the “ones” remain mainly unchanged. On the other hand, for a constant value of the filter offset, Δf = 200 GHz, we have measured output versus input proportion of the ghost-pulse energy with respect to the “ones” energy. The experimental results reported in Fig. 4(b) show that the ghost-pulses are efficiently suppressed even for high input energies. More precisely, the output ghost energy proportion remains less than 1% as long as the input ghost energy proportion is less than about 20 %. Let us note that the threshold for ghost pulse suppression can be simply adjusted by changing the filter frequency detuning. As expected, the transfer function of the similariton generator is nonlinear so that only high-power pulses are transmitted. Moreover, we verify from Fig. 4(b) that when the ghost energy becomes comparable to the “ones” energy, the ghost pulses are totally transmitted by the similariton generator.

In conclusion, we have presented an all-optical regeneration technique based on similariton generation. This technique has been successfully applied to suppress noise and ghost pulses in a 40-Gb/s pulse train. Theoretical predictions were confirmed by experimental results. An interesting straightforward extension of our work could be to use the similaritons for PRBS regeneration at the end of an experimental telecommunication line.

This work was supported by the Conseil Régional de Bourgogne, the Centre National de la Recherche Scientifique (CNRS) and the Ministère de la Recherche et des Nouvelles Technologies (MRNT). C. Finot’s e-mail address is Christophe.Finot@u-bourgogne.fr.

References

1. R. J. Essiambre, B. Mikkelsen, and G. Raybon, Electron. Lett. **35**, 1576 (1999).
2. W. Wang, H. N. Poulsen, L. Rau, C. Hsu-Feng, J. E. Bowers, D. J. Blumenthal, and L. Gruner-Nielsen, IEEE Photon. Technol. Lett. **15**, 1416 (2003).
3. P. V. Mamyshev, in *Proceedings of European Conference on Optical Communication*, ECOC'98, (Institute of Electrical and Electronics Engineering, Madrid, Spain, 1998) **1**, pp. 475-476.
4. J. T. Mok, J. L. Blows, and B. J. Eggleton, Opt. Express **12**, 4411 (2004).
5. T.-H. Her, G. Raybon, and C. Headley, IEEE Photon. Technol. Lett. **16**, 200 (2004).
6. E. Ciaramella and S. Trillo, IEEE Photon. Technol. Lett. **12**, 849 (2000).
7. A. Bogoni, P. Ghelfi, M. Scaffardi, and L. Poti, IEEE J. Select. Top. Quantum Electron. **10**, 192 (2004).
8. M. E. Fermann, V. I. Kruglov, B.C. Thomsen, J. M. Dudley, and J. D. Harvey, Phys. Rev. Lett. **84**, 6010 (2000).
9. J. Limpert, T. Schreiber, T. Clausnitzer, K. Zöllner, H. -J. Fuchs, E. -B Bley, H. Zellmer, and A. Tünnermann, Opt. Express **10**, 628 (2002).
10. C. Finot, G. Millot, C. Billet, and J. M. Dudley, Opt. Express **11**, 1547 (2003).
11. C. Finot and G. Millot, Opt. Express **12**, 5104 (2004.
12. F.Ö. Ilday, J.R. Buckley, W. G. Clark and F.W. Wise, Phys. Rev. Lett. **92**, 213902 (2004).
13. V. I. Kruglov, A. C. Peacock, J. M. Dudley, and J. D. Harvey, J. Opt. Soc. Am. B **19**, 461 (2002).
14. C. Finot, G. Millot, and J. M. Dudley, Opt. Lett. **29**, 2533 (2004).
15. S. Pitois, J. Fatome, and G. Millot, Opt. Lett. **27**, 1729 (2002).

Figure captions

Fig. 1. Illustration of the spectral broadening associated with parabolic pulse generation. Intensity spectra in a logarithmic scale of a 40-GHz pulse train: (a1) at the fiber input, (b1) and (c1) after amplification in the NZ-DSF for P_{av} = 40 mW and 230 mW, respectively. The dashed line represents the transmission profile of the optical filter. (a2), (b2) and (c2) represent the corresponding pulse trains.

Fig. 2. Eye diagrams for a 40-Gb/s pseudo-random bit sequence. (a) initial pulse train, (b) after propagation through a transmission line, (c) after self-similar amplification in the NZ-DSF, and (d) after filtering with a filter offset of 100 GHz.

Fig. 3. Experimental set-up. VA: variable attenuator, EDFA: erbium doped fiber amplifier, BPF: optical bandpass filter.

Fig. 4. (a) Experimental autocorrelation traces of the 40-Gb/s pulse train at the Raman amplifier input (circles) and output for different values of the filter offset. (b) Experimental output versus input proportion of ghost pulse energy for a filter offset of 200 GHz.

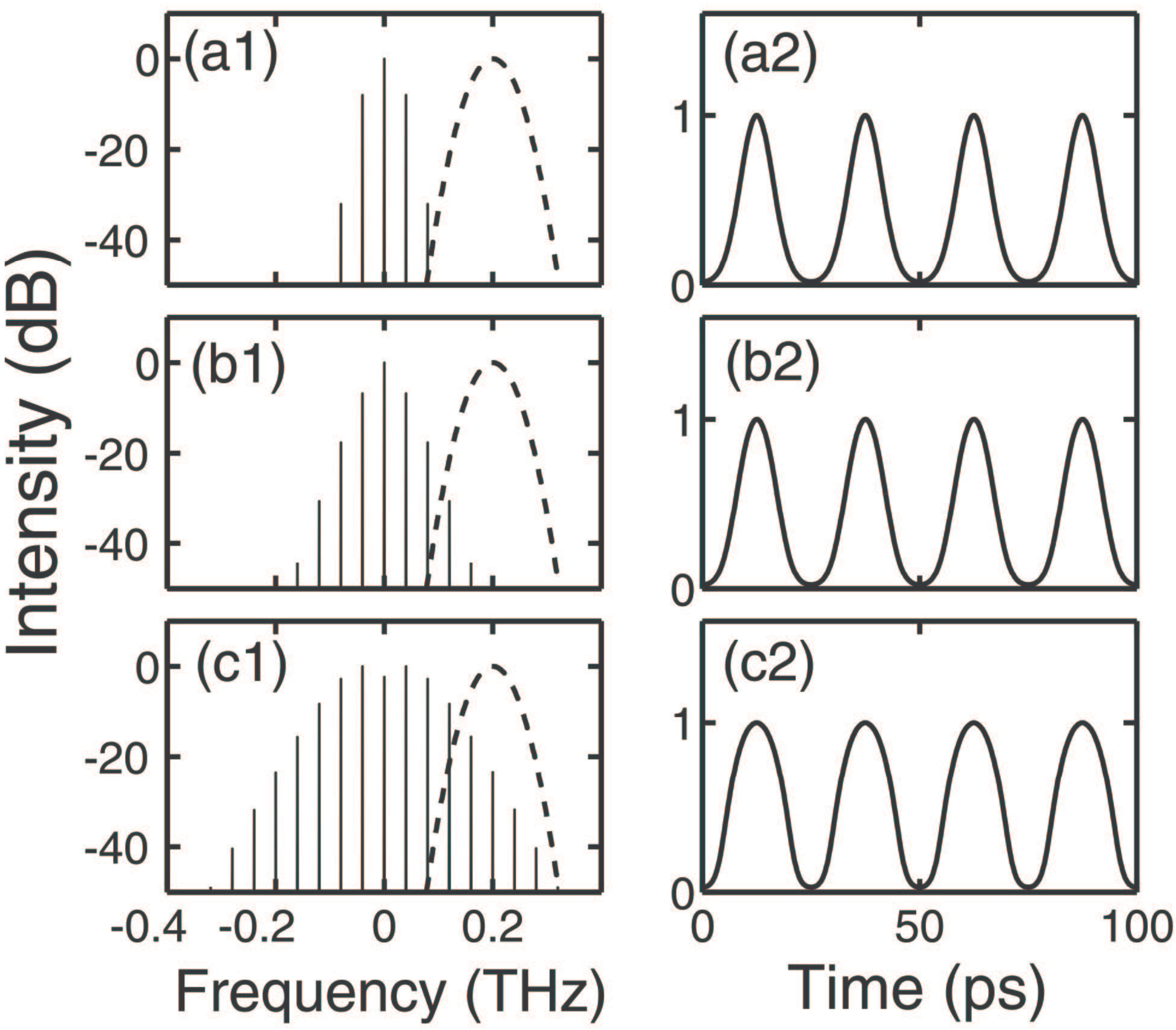

Intensity (dB)
(a1)
(b1)
(c1)
0
-20
-40
-0.4
-0.2
0
0.2
Frequency (THz)
(a2)
(b2)
(c2)
1
0
50
100
Time (ps)

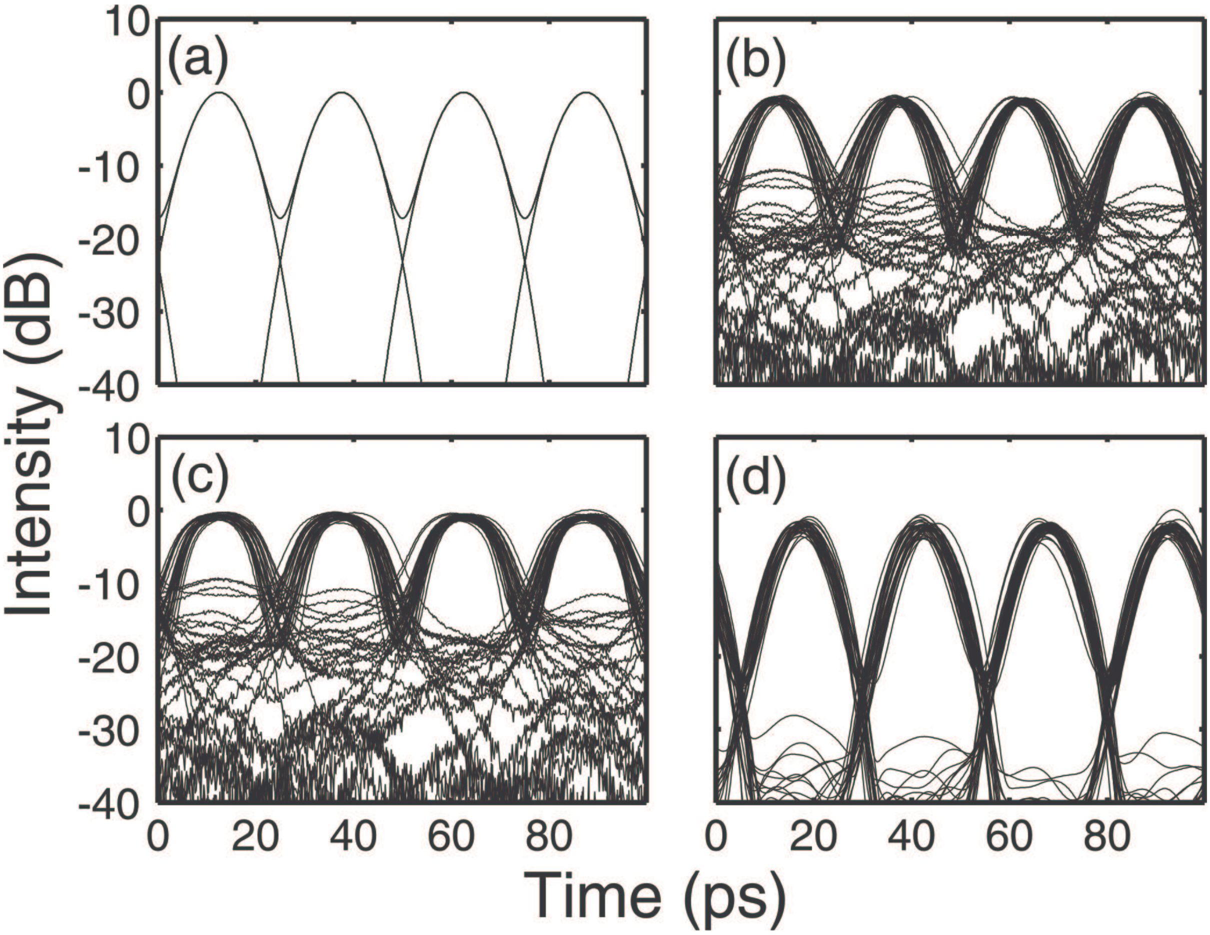
(a)
(b)
(c)
(d)
Intensity (dB)
Time (ps)
10
0
-10
-20
-30
-40
0
20
40
60
80

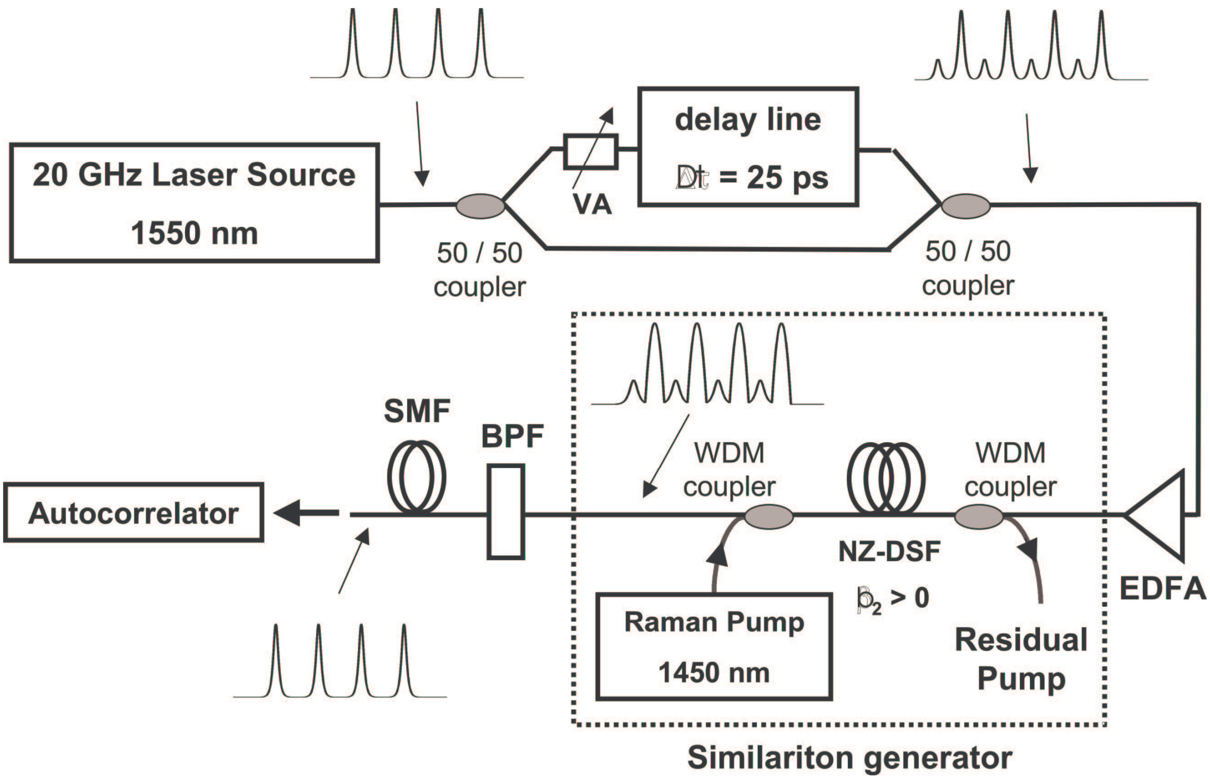
20 GHz Laser Source
1550 nm
delay line
Dt = 25 ps
VA
50 / 50
coupler
50 / 50
coupler
SMF
BPF
Autocorrelator
WDM
coupler
WDM
coupler
NZ-DSF
b2 > 0
Raman Pump
1450 nm
Residual
Pump
EDFA
Similariton generator

Finot, Pitois, Millot **Fig. 4**